Title

DUOX expression in human keratinocytes and bronchial epithelial cells: Influence of vanadate

Authors

Hill, Thomas
Rice, Robert H

Publication Date

2018-02-01

DOI

10.1016/j.tiv.2017.10.010

Peer reviewed

HHS Public Access

Author manuscript

Toxicol In Vitro. Author manuscript; available in PMC 2019 February 01.

Published in final edited form as:

Toxicol In Vitro. 2018 February ; 46: 257–264. doi:10.1016/j.tiv.2017.10.010.

DUOX Expression in Human Keratinocytes and Bronchial Epithelial Cells: Influence of Vanadate

Thomas Hill III and **Robert H. Rice***

Department of Environmental Toxicology, University of California at Davis

Abstract

Dual oxygenases (DUOX) 1 and 2, expressed in many animal tissues, participate in host defense at mucosal surfaces and may have important signaling roles through generation of reactive oxygen. Present work addresses their expression in cultured human epidermal keratinocytes and effects of cytokines and metal/metalloid compounds. Both DUOX1 and 2 were expressed at much higher levels after confluence than in the preconfluent state. Maximal DUOX1 mRNA levels were 50 fold those of DUOX2. DUOX1 and 2 were induced ≈3 fold by interleukin 4, but only DUOX1 was induced by interferon gamma (IFNγ). In human bronchial HBE1 cells, by contrast, interleukin 4 induced only DUOX 1, and IFNγ induced only DUOX2. A survey in the keratinocytes of metal/metalloid compounds showed that arsenite, antimonite, chromate, cadmium, copper, lead and vanadate suppressed DUOX1 levels but did not prevent interleukin 4 stimulation. Effects on DUOX2 were less dramatic, except that vanadate potentiated the stimulation by IFNγ up to 7 fold. The results indicate that epithelial cell types of different tissue origins can differ in their cytokine regulation and that epidermal cells can exhibit striking alterations in response due to certain metal/metalloid exposures.

Keywords

DUOX; Human epidermal keratinocytes; Human bronchial cells; Interferon γ; Interleukin 4; Vanadate

Introduction

Exposure to reactive oxygen species (ROS) from radiation or exogenous chemicals is well known to have adverse biological effects. However, in addition to causing disease when it is present in excess, ROS generated endogenously can have important roles in cell signaling, homeostatic and defensive functions (Lambeth and Neish, 2014). The regulated production of ROS by the NADPH:O2 oxidoreductase (NOX) family of membrane proteins is ubiquitous in both the plant and animal kingdoms (Bedard et al., 2007; Leto and Geiszt,

*Corresponding Author R. H. Rice, Department of Environmental Toxicology, University of California, One Shields Avenue, Davis, CA 95616-8588 USA; Tel 530-752-5176; Fax 530-752-3394; rhrice@ucdavis.edu.

2006; Ritsick et al., 2004; Sumimoto, 2008). Illustrating a role in host defense in humans, the loss of superoxide production in phagocytic cells in X-linked chronic granulomatous disease, a syndrome characterized by frequent microbial infections, led to discovery of a deficiency in NOX2 (gp91phox) (Orkin, 1989; Segal, 1988). This finding prompted identification of 5 NOX enzymes (NOX1- 5) and the related DUOX1 and 2.

Like the NOX enzymes, dual oxygenases (DUOX) 1 and 2 are expressed in many animal tissues and have diverse proposed roles. For example, they generate hydrogen peroxide used by lactoperoxidase in host defense at mucosal surfaces (Geiszt et al., 2003), including the airways (Moskwa et al., 2007). DUOX2 was identified as the enzyme that catalyzes incorporation of iodine into thyroid hormone (Dupuy et al., 1999) and is lacking in congenital hypothyroidism (Moreno et al., 2002). To become active and localized in the plasma membrane, these enzymes form heterodimers with transcriptionally linked DUOXA1 and DUOXA2 proteins, respectively (Grasberger and Refetoff, 2006). Distinct from NOX1-4, and noteworthy due to the influence of calcium on cell differentiation, they have Ca++-binding intracellular EF-hand motifs that permit regulation by internal calcium levels (Ameziane-El-Hassani et al., 2005).

Previous work has shown that DUOX1 expression in cultured normal human epidermal keratinocytes is largely responsible for hydrogen peroxide production, and that its expression (along with numerous differentiation markers) is increased with elevated calcium concentration in the medium. Moreover, its inhibition using diphelyleneiodonium (an inhibitor of NOX and DUOX enzymes) or knock down using siRNA suppresses levels of a number of differentiation markers, including loricrin, filaggrin, keratins 1 and 10, desmocollin 1, and desmoglein 1, that are important for proper barrier function (Choi et al., 2014). In similar cultures, treatment with the Th2 cytokines IL4 or IL13 induced some 200 genes, including DUOX1 by 2–3 fold. The increase in DUOX1 increased hydrogen peroxide, oxidation of protein tyrosine phosphatase 1B and phosphorylation of STAT6 (Hirakawa et al., 2011). This finding suggested DUOX1 could participate in a positive feedback loop and synergize with TNFα and other cytokines in the epidermis. As an example, DUOX1 can regulate Src and EGF receptor in a ligand independent manner in the respiratory tract (Heppner et al., 2016).

Building on these results, present work explores the response of DUOX1 and 2 to representative Th1 and Th2 cytokines in culture, contrasting the effects in keratinocytes with those in bronchial epithelial cells (HBE1). The results in these model cell lines, minimally deviated from normal, provide a foundation for examining perturbation of DUOX expression by metal/metalloid compounds often present from environmental or occupational exposures. Certain metal/metalloid contaminants (e.g., arsenic) in drinking water have been shown to affect keratinocyte differentiation and signal transduction mediators (Paul et al., 2007; Reznikova et al., 2009). Several studies report that arsenic action in endothelium, characterized by ROS generation, is mediated by NOX induction or activation but have not touched on possible DUOX contributions (Pan et al., 2011; Straub et al., 2008). Arsenic exposure through drinking water is a worldwide problem (Nordstrom, 2002), affecting millions of people, and perhaps represents the largest mass poisoning in world history (Bhattacharjee, 2007). Analysis of geothermal waters in pristine wilderness areas of the

United States suggest that arsenic remains a concern in many localities, and that discharge of these compounds may be a significant health hazard to downstream communities or geothermal energy personnel (Planer-Friedrich et al., 2007). Arsenic contamination clearly remains an important issue even in developed nations and, ironically, the projected expansion of oil shale extraction and energy alternatives such as geothermal power may increase the risk of exposure (Mitchell et al., 2011).

Additional studies have indicated air or water pollutants from mining activity that contain metal ions and oxyanions such as cadmium, copper, chromate, or vanadate may also function as keratinocyte toxicants through generation of ROS (Gummow et al., 2006; Kawata et al., 2007; Wang et al., 2003). Metals from such airborne sources are well known contributors to hypersensitivity responses of the airways and the skin (Godri Pollitt et al., 2016; Swinnen and Goossens, 2013). Exposure to particulates containing antimony, arsenic, cadmium, chromium, copper, lead, vanadium, zinc and other metals and metalloids occurs from traffic emissions, petroleum refineries and fuel combustion. Very high environmental levels are reached particularly in developing countries in general (Shakir et al., 2017) and especially in areas near electronic waste processing (Song and Li, 2015).

Methods

Cell culture

The papilloma virus E6/E7-immortalized human bronchial epithelial line HBE1 was provided by Dr. J. Yankaskas (Yankaskas et al., 1993). The cells were maintained in Ham's F12/Hepes/DMEM supplemented with insulin (2 μg/ml), transferrin (2.5 μg/ml), epidermal growth factor (10 ng/ml), dexamethasone (0.05 μM), cholera toxin (10 ng/ml), bovine hypothalamic extract (50 μg/ml) and plasmocin (2.5 μg/ml). Spontaneously immortalized human epidermal keratinocytes (SIK), passages 23–29, were co-cultured with a lethally irradiated 3T3 feeder layer in a 2:1 mixture of DMEM and F12 media supplemented with fetal bovine serum (5%), hydrocortisone (0.4 μg/mL), insulin (5 μg/mL), transferrin (5 μg/mL), triiodothyronine (20 pM), and adenine (0.18 mM) (Rice et al., 1993). Epidermal growth factor (10 nM) was added at the first medium change. Newly confluent cultures were trypsinized, diluted 1:4 into 12 well cell culture dishes (Greiner Bio-One International AG, Frickenhausen, Germany) and grown until approximately 90% confluent prior to cytokine treatments or chemical exposures.

Cytokine Treatments

Recombinant human IFNγ and IL4 (R&D Systems, Inc., Minneapolis, MN) were dissolved in sterile phosphate-buffered saline (PBS) with 1% bovine serum albumin (BSA). Serial dilutions in medium were added to the wells, and each treatment was repeated in triplicate. Cytokine treatments were performed at their EC50 concentrations determined in initial experiments (Figures 3 and 4) for 24 hours. Control wells were treated with 75 μl of PBS: 1% BSA vehicle in 1.5 ml of medium. Test and control treatments were set up using a simple Latin Square design.

Chemical exposure of cultures

Stock solutions of the agents employed ($NaAsO_2$, K_2CrO_4, Na_3VO_4, $ZnSO_4$, $CuSO_4$, $CdCl_2$, $Pb(NO_3)_2$, and potassium antimony tartrate) in water were sterile filtered and stored at 4°C until use. Concentrations employed for the screen were close to the EPA maximal drinking water contaminant limits (Cr, Cu, Zn) or observed in contaminated watersheds or water supplies (As, Cd, Pb, Sb). Hemin was prepared in dimethylsulfoxide (DMSO) as a 1000× stock solution. Cells were exposed to agents for 3 days prior to and during cytokine or dimethylthiourea (DMTU) addition. The medium was changed on days one and three, and cultures were harvested at the end of the third day. DMTU (30 mM) was added at the start of day 3 and followed by cytokine addition one hour later. Statistical analysis on 4–6 biological replicates was performed, as indicated in the figure legend, by t-test or one way ANOVA (with Bonferroni corrections) using STATA/SE9.2 software for Windows.

RNA Isolation and Quantitation

RNA was isolated using Trizol (Invitrogen, Carlsbad, CA). cDNA was transcribed from 2–3 μg of total RNA for each sample using oligo-dT and random primers at 25°C for 10 min, followed by PCR amplification with MultiScribe-reverse transcriptase (ABI, Austin TX) for 60 min in 20 μl reaction volumes. The cDNA stock was then diluted 1:5 in nuclease free water for quantitative, real time PCR (QPCR). The QPCR was performed on an ABI PRISM© 7900HT Sequence Detection System (Applied Biosystems, Inc., Foster City, CA) using gene specific, intron-spanning primers for Duox1, Duox2, and β-actin as previously described (Harper et al., 2005). Reactions were carried out in 384-well optical reaction plates with 10 μl final volumes using SYBR®GreenER™ qPCR Supermix (Invitrogen, Carlsbad, CA). Reactions were carried out in triplicate for each of the three biological replicates; both melting curve analysis and non-template controls were utilized to assure amplification specificity. Ct values ranged from 20 to 30 in figures 3–9; those for DUOX induction were normalized to those of β-actin, and calculations of fold induction relative to controls (ΔΔCt) were performed (Bookout et al., 2007). Pharmacokinetic derivations and modeling were performed using WinNon-Lin (Pharsight Software, Mountain View, CA) and SigmaPlot (Systat Software Inc., San Jose, CA). Values illustrated are means and standard deviations across the biological replicates.

Next Generation Sequencing

Total messenger RNA (mRNA) was prepared using Trizol reagent (Thermo–Fisher Scientific) from two experiments, one of which has been previously reported (Phillips et al., 2016), each with two independent samples. Sequencing libraries were prepared using an Illumina TrueSeq mRNA sample preparation kit. Messenger RNA was purified and converted to double-stranded complementary DNA (cDNA). Adapters and specific indexes were added to each sample. RNA sequencing was performed on a HiSEqn 2500 sequencer analyzer (Illumina, San Diego, CA). Sequencing reads were analyzed using CLCBio Genomic Workbench software (CLC Bio, Aarhus, Denmark) (Wickramasinghe et al., 2014). Quality control (QC) analysis was performed using the application NGS quality control tool of CLC Genomics Workbench software (CLC Bio) (Cánovas et al., 2013). Sequenced single reads (100 bp) were assembled against the annotated human reference genome (release 80)

(ftp://ftp.ensembl.org/pub/release-80/genbank/homo_sapiens/). Data were normalized by calculating the 'reads per kilobase per million mapped reads' (RPKM) for each gene.

Results

Endogenously controlled expression of DUOX1 and DUOX2 in keratinocytes was found to be strongly influenced by the growth state of the cells. When growing SIK cultures were held past confluence, they became increasingly differentiated, and the expression of both DUOX genes was considerably induced (Figure 1). Although the degree of DUOX2 induction was several fold higher than DUOX1, the level of expression of DUOX1 was at least 50 fold that of DUOX2 after a week at confluence (Figure 2). As shown in Figure 2A, DUOX1 and DUOXA1, genetically linked, were expressed at similar levels, while DUOX2 and DUOXA2, also genetically linked, were expressed at similar but much lower levels (Fig 2B). The latter were expressed at much higher levels than NOX1, 4, 5 and NOXO1, while NOXA1 was expressed at a level 4 fold that of DUOX2. NOX 2 and 3 were not detected.

Cytokine responses of human keratinocytes in comparison with bronchial epithelial cells in culture

To determine how DUOX gene induction is directed by a Th2 cytokine, the concentration dependence of DUOX1 and DUOX2 on IL-4 was characterized in HBE1 and SIK cultures. Treatment with IL4 induced both DUOX1 and DUOX2 mRNAs in SIK cultures (Figure 3A). Maximal inductions of 2–3 fold (DUOX1) and 3–4 fold (DUOX2) occurred in the range of 3–30 ng/ml with EC50 values in the vicinity of 10 ng/ml. By contrast, treatment of HBE1 cells induced only DUOX1 (EC50 10 ng/ml); maximal levels of 5–6 fold above uninduced cultures were attained at ≥20 ng/ml (Fig 3B). Treatment at >60 ng/ml resulted in considerable cell lysis.

The effects of Th1 cytokines were characterized in HBE1 and SIK cultures using IFNγ. The cell lines responded similarly, but with discrete sensitivities. Continuous exposure to IFNγ consistently induced only DUOX2 in SIK cultures, whereas clear evidence for DUOX1 induction was not observed (Fig 4A). Maximal levels of 3.5 fold those in untreated cultures were attained at ≈1000 ng/ml concentrations with an EC50 value of 50 ng/ml. By contrast, treatment of HBE1 cells induced DUOX2 by 25 fold above untreated levels at 600 ng/ml and nearly 50 fold by 1700 ng/ml (Fig 4B); no induction of DUOX1 was observed.

To approximate the "burst-release" of cytokines *in vivo*, both cell lines were treated with a two hour pulse-dose at the EC50 derived for each cytokine, and the response was compared with continuous exposure at the same dose. Treatment of SIK cultures for either 2 or 24 hr with IFNγ showed no induction of DUOX1 (Fig 5A), while DUOX2 was induced by 24 but not 2 hr of treatment with either IFNγ or IL4. By contrast, DUOX2 was induced in HBE1 cells as well or better by 2 hr as by 24 hr of exposure (Fig 5B).

To approximate *in vivo* impacts of cytokine balance on DUOX induction, cells were treated with the Th1 cytokine IL4 at its EC50 with simultaneous exposure to an increasing dose of the Th2 cytokine IFNγ. In SIK cultures, IFNγ at each dose suppressed DUOX1 induction, but DUOX2 induction appeared to be only nominally affected (Fig 6A). By contrast,

DUOX1 was strongly suppressed in HBE1 cells with an IC50 for IFNγ of ≈100 ng/ml and >80% suppression at 5000 ng/ml. Furthermore, DUOX2 was induced by IFNγ only to ≈10% of the level seen in the absence of IL4 (Fig 6B).

Vanadate augmentation of DUOX2 induction by IFNγ

SIK cultures were treated with a selection of metal/metalloid compounds for 3 days at biologically relevant concentrations and then for a day with either IFNγ or IL4 near their EC50 values determined above. As shown in Fig 7A, each of the metal/metalloid treatments (except Zn, not tested) substantially suppressed the level of DUOX1, whereas IL4 generally stimulated DUOX1 similarly in each case. Except for vanadate, the net effect of combined treatment with metal/metalloid and IL4 was a DUOX1 induction close to that of untreated cultures. The similarity of this suppression to that of arsenite and antimonite in the absence of IL4 was also seen for DUOXA1 but not for DUOX2, DUOXA2 or other members of the NOX family (Fig 2). Treatment of the cultures with metals/metalloids generally had less effect on DUOX2 than on DUOX1 and, except for Zn and antimonite, did not prevent at least partial induction by IFNγ (Fig 7B). A dramatic contrast was the 15 fold induction by IFNγ in the presence of vanadate compared to 4–5 fold induction by IFNγ alone. The concentration dependence of this vanadate effect was then explored. As seen in Fig 8, amplification of the IFNγ stimulation was obvious from 2–15 μM. The increase did not plateau at the maximal concentration tested (15 μM), but higher concentrations were not tested due to likely toxicity. Although 15 μM is below the level of concern for drinking water calculated in a recent EPA study (Benson et al., 2017), vanadate >5 μM is known to arrest keratinocyte growth in culture (Rea and Rice, 2001).

The effect of the ROS quenching agent dimethylthiourea (DMTU) on the cytokine induction of DUOX isoforms in SIK cultures was examined in the presence and absence of vanadate. Panel 9A shows the induction of DUOX2 by IFNγ, nearly 8 fold, and its further 4 fold augmentation by vanadate. When DMTU was included in the medium, however, little DUOX2 stimulation occurred. In parallel experiments with IL4 stimulation (Fig 9B), vanadate was similarly effective in augmenting DUOX2 induction. However, DMTU had little if any effect on the induction.

Discussion

Present work confirms that DUOX1 is expressed at much higher levels in human epidermal keratinocytes than is DUOX2 and also shows that levels of genetically linked DUOXA1 and A2 are comparable to DUOX1 and DUOX2, respectively. Moreover, it became evident that an increase in levels of DUOX1 and 2 occurred in the cells as they increased in degree of differentiation after confluence. The fold increase was particularly pronounced for DUOX2. That the activity of DUOX enzymes is stimulated by increased calcium through their EF-hand motifs suggests their production of hydrogen peroxide increases with the differentiated state of the cells as their expression increases. A consequence of such production appears to be stimulation of the differentiation state (Choi et al., 2014), although another, possibly larger, contribution of ROS with this effect appears to arise through leakage from the mitochondrial electron transport chain (Hamanaka et al., 2013). Consistent with these

results, a contribution of oxygen to increasing the state of differentiation is also seen in the lower degree of differentiation in keratinocyte cultures propagated in lower oxygen tension (Ngo et al., 2007).

Judging by mRNA amounts, DUOX1 appears to dominate; however, functional contributions of DUOX2 and NOX enzymes cannot be ruled out. For example, NOX1 and lactoperoxidase are considerably stimulated in keratinocytes by ionizing radiation (Dong et al., 2011). Despite its low level ordinarily, NOX1 is a major source of ROS in keratinocytes irradiated with ultraviolet light (Valencia and Kochevar, 2008). Under that condition, the presence of lactoperoxidase (normally not present) could enhance host defense toward microbes by ROS from DUOX and NOX activity.

The present study of DUOX induction by cytokines indicates it can occur by receptor-mediated processes in keratinocytes as shown previously in airway epithelial cells (Harper et al., 2005; Hill et al., 2010). A novel finding in keratinocytes is the IL4 induction of both DUOX1 and DUOX2. The keratinocytes differed from HBE1 cells in not responding to a 2 hr pulse of IL4. A second novel observation is the IFNγ suppression of the keratinocyte response to IL4 for both DUOX1 and the modulation of DUOX2 expression in HBE1 cells in the presence of IL4. These findings, providing a clear description of DUOX/cytokine dose response relations, are evidence for tissue-specific cytokine cross-talk. Along with the traditional association of DUOX1 with proliferative cell behavior/signaling and DUOX2 with local inflammatory activity, these data suggest that a balanced protective response is reliant on competent gene induction pathways for both isoforms. Thus, disease states or environmental exposures that alter the Th1/Th2 levels and their balance in the respiratory tract could alter DUOX1 and 2 levels and likely impair natural host defense mechanisms. Similar perturbations of DUOX expression in the skin could lead to epidermal barrier defects and enhanced penetration by contact agents or environmental toxicants.

As the major extrapulmonary barrier to the environment, the epidermis is frequently subject to metal/metalloid exposure. Present findings emphasize the potential perturbation that could result. That arsenite and antimonite had essentially the same effect emphasizes recent evidence these contaminants have nearly identical biological activities (Phillips et al., 2016). Although DUOX2 is much less prevalent than DUOX1 in the keratinocytes, its functional contribution cannot be discounted. Vanadate augmentation of DUOX2 induction provides insight into its regulation in the skin. The powerful prevention of stimulation by the radical scavenger DMTU suggests ROS participate in signaling processes driving induction. That DMTU treatment did not affect vanadate stimulation suggests the latter's well-known action as a tyrosine phosphatase inhibitor (Gordon, 1991) mediates its effect. This scenario illustrates a way in which vanadate exposure could interact in concert with the DUOX product, hydrogen peroxide, in feedback loops augmenting cytokine action in the skin (Hirakawa et al., 2011). Previous studies have shown that vanadate prolongs IFNγ activation of STAT1 phosphorylation by inhibiting a protein tyrosine phosphatase in the nucleus of fibroblasts (David et al., 1993; Haspel and Darnell, 1999). Despite some progress in understanding the roles of protein tyrosine phosphatases in such signaling, many details, including identifying responsible phosphatases, are important topics for future research (Böhmer and Friedrich, 2014).

Acknowledgments

We thank Qin Qin and Dr. Marjorie A. Phillips for expert assistance overall, Drs. Angela Cánovas and Juan Medrano for helping generate next generation sequencing data, Dr. Jerold A. Last for valuable advice, Dr. Alan R. Buckpitt for glutathione measurements and the Real-time PCR Research and Diagnostics Core Facility at the UC Davis School of Veterinary Medicine for QPCR data collection. This work was supported by training grant T32 ES07059, NIH grants R01 HL085311 (R. W. Harper) and P42 ES04699 (R. H. Rice), and a Battelle Student Research Award (T. Hill) from the Dermal Toxicology Specialty Section of the Society of Toxicology. The content is solely the responsibility of the authors and does not necessarily represent the official views of the NIEHS/NIH.

References

Ameziane-El-Hassani R, Morand S, Boucher JL, Frapart YM, Apostolou D, Agnandji D, Gnidehou S, Ohayon R, Noël-Hudson MS, Francon J, Lalaoui K, Virion A, Dupuy C. Dual oxidase-2 has an intrinsic Ca2+-dependent H2O2-generating activity. J Biol Chem. 2005; 280:30046–30054. [PubMed: 15972824]

Bedard K, Lardy B, Krause KH. NOX family NADPH oxidases: not just in mammals. Biochimie. 2007; 89:1107–1112. [PubMed: 17400358]

Benson R, Conerly OD, Sander W, Batt AL, Boone JS, Furlong ET, Glassmeyer ST, Kolpin DW, Mash HE, Schenck KM, Simmons JE. Human health screening and public health significance of contaminants of emerging concern detected in public water supplies. Sci Total Environ. 2017; 579:1643–1648. [PubMed: 28040195]

Bhattacharjee Y. A sluggish response to humanity's biggest mass poisoning. Science. 2007; 315:1659–1661. [PubMed: 17379786]

Böhmer FD, Friedrich K. Protein tyrosine phosphatases as wardens of STAT signaling. JAKSTAT. 2014; 3(1):e28087. [PubMed: 24778927]

Bookout, AL., Cummins, CL., Mangelsdorf, DJ., Pesola, JM., Kramer, MF. High-throughput real-time quantitative reverse transcription PCR. In: Ausubel, FM.Brent, R.Kingston, RE.Moore, DD., Seidman, JG., editors. Current Protocols in Molecular Biology. 20. John Wiley and Sons, Inc; Hoboken, NJ: 2007. p. 1-28.

Cánovas A, Rincón G, Islas-Trejo A, Jimenez-Flores R, Laubscher A, Medrano JF. RNA sequencing to study gene expression and single nucleotide polymorphism variation associated with citrate content in cow milk. J Dairy Sci. 2013; 96:2637–2648. [PubMed: 23403202]

Choi H, Park JY, Kim HJ, Noh M, Ueyama T, Bae Y, Lee TR, Shin DW. Hydrogen peroxide generated by DUOX1 regulates the expression levels of specific differentiation markers in normal human keratinocytes. J Dermatol Sc. 2014; 74:56–63. [PubMed: 24332816]

David M, Grimley PM, Finbloom DS, Larner AC. A nuclear tyrosine phosphatase downregulates interferon-induced gene expression. Molec Cell Biol. 1993; 13:7515–7521. [PubMed: 8246969]

Dong Q, Oh JE, Chen W, Kim R, Kim RH, Shin KH, McBride WH, Park NH, Kang MK. Radioprotective effects of Bmi-1 involve epigenetic silencing of oxidase genes and enhanced DNA repair in normal human keratinocytes. J Invest Dermatol. 2011; 131:1216–1225. [PubMed: 21307872]

Dupuy C, Ohayon R, Valent A, Noël-Hudson MS, Dème D, Virion A. Purification of a novel flavoprotein involved in the thyroid NADPH oxidase. Cloning of the porcine and human cDNAs. J Biol Chem. 1999; 274:37265–37269. [PubMed: 10601291]

Geiszt M, Witta J, Baffi J, Lekstrom K, Leto TL. Dual oxidases represent novel hydrogen peroxide sources supporting mucosal surface host defense. FASEB J. 2003; 17:1502–1504. [PubMed: 12824283]

Godri Pollitt KJ, Maikawa CL, Wheeler AJ, Weichenthal S, Dobbin NA, Liu L, Goldberg MS. Trace metal exposure is associated with increased exhaled nitric oxide in asthmatic children. Environ Health. 2016; 15:94. [PubMed: 27586245]

Gordon JA. Use of vanadate as protein-phosphotyrosine phosphatase inhibitor. Meth Enzymol. 1991; 201:477–482. [PubMed: 1943774]

Grasberger H, Refetoff S. Identification of the maturation factor for dual oxidase. Evolution of an eukaryotic operon equivalent. J Biol Chem. 2006; 281:18269–18272. [PubMed: 16651268]

Gummow B, Kirsten WF, Gummow RJ, Heesterbeek JA. A stochastic exposure assessment model to estimate vanadium intake by beef cattle used as sentinels for the South African vanadium mining industry. Prevent Vet Med. 2006; 76:167–184.

Hamanaka RB, Glasauer A, Hoover P, Yang S, Blatt H, Mullen AR, Getsios S, Gottardi CJ, DeBerardinis RJ, Lavker RM, Chandel NS. Mitochondrial reactive oxygen species promote epidermal differentiation and hair follicle development. Science Signaling. 2013; 6(261):ra8. [PubMed: 23386745]

Harper RW, Xu C, Eiserich JP, Chen Y, Kao CY, Thai P, Setiadi H, Wu R. Differential regulation of dual NADPH osidases/peroxidases, Duox1 and Duox2, by Th1 and Th2 cytokines in respiratory tract epithelium. FEBS Lett. 2005; 579:4911–4917. [PubMed: 16111680]

Haspel RL, Darnell JEJ. A nuclear protein tyrosine phosphatase is required for the inactivation of Stat1. Proceedings of the National Academy of Science USA. 1999; 96:10188–10193.

Heppner DE, Hristova M, Dustin CM, Danyal K, Habibovic A, van der Vliet A. The NADPH oxidases DUOX1 and NOX2 play distinct roles in redox regulation of epidermal growth factor receptor signaling. J Biol Chem. 2016; 291:23282–23293. [PubMed: 27650496]

Hill TI, Xu C, Harper RW. IFNgamma mediates DUOX2 expression via a STAT-independent signaling pathway. Biochem Biophys Res Commun. 2010; 395:270–274. [PubMed: 20381453]

Hirakawa S, Saito R, Ohara H, Okuyama R, Aiba S. Dual oxidase 1 induced by Th2 cytokines promotes STAT6 phosphorylation via oxidative inactivation of protein tyrosine phosphatase 1B in human epidermal keratinocytes. J Immunol. 2011; 186:4762–4770. [PubMed: 21411736]

Kawata K, Yokoo H, Shimazaki R, Okabe S. Classification of heavy-metal toxicity by human DNA microarray analysis. Environ Sci Technol. 2007; 41:3769–3774. [PubMed: 17547211]

Lambeth JD, Neish AS. Nox enzymes and new thinking on reactive oxygen: a double-edged sword revisited. Ann Rev Pathol. 2014; 9:119–145. [PubMed: 24050626]

Leto TL, Geiszt M. Role of Nox family NADPH oxidases in host defense. Antiox Redox Signaling. 2006; 8:1549–1561.

Mitchell W, Goldberg S, Al-Abadleh HA. In situ ATR-FTIR and surface complexation modeling studies on the adsorption of dimethylarsinic acid and p-arsanilic acid on iron-(oxyhydr)oxides. J Colloid Interface Sci. 2011; 358:534–540. [PubMed: 21457993]

Moreno JC, Bikker H, Kempers MJ, van Trotsenburg AS, Baas F, de Vijlder JJ, Vulsma T, Ris-Stalpers C. Inactivating mutations in the gene for thyroid oxidase 2 (THOX2) and congenital hypothyroidism. New England J Med. 2002; 347:95–102. [PubMed: 12110737]

Moskwa P, Lorentzen D, Excoffon KJ, Zabner J, McCray PBJ, Nauseef WM, Dupuy C, Bánfi B. A novel host defense system of airways is defective in cystic fibrosis. American Journal of Resp Crit Care Med. 2007; 175:174–183.

Ngo MA, Sinitsyna NN, Qin Q, Rice RH. Oxygen dependent differentiation of human keratinocytes. J Invest Dermatol. 2007; 126:2507–2515.

Nordstrom DK. Worldwide occurrences of arsenic in ground water. Science. 2002; 296:2143–2144. [PubMed: 12077387]

Orkin SH. Molecular genetics of chronic granulomatous disease. Ann Rev Immunol. 1989; 7:277–307. [PubMed: 2523713]

Pan X, Dai Y, Li X, Niu N, Li W, Liu F, Zhao Y, Yu Z. Inhibition of arsenic induced-rat liver injury by grape seed exact through suppression of NADPH oxidase and TGF-beta/Smad activation. Toxicol Appl Pharmacol. 2011; 254:323–331. [PubMed: 21605584]

Paul DS, Harmon AW, Devesa V, Thomas DJ, Styblo M. Molecular mechanisms of the diabetogenic effects of arsenic: inhibition of insulin signaling by arsenite and methylarsonous acid. Environ Health Perspect. 2007; 115:734–742. [PubMed: 17520061]

Phillips MA, Cánovas A, Wu PW, Islas-Trejo A, Medrano JF, Rice RH. Parallel responses of human epidermal keratinocytes to inorganic SbIII and AsIII. Environ Chem. 2016; 13:963–970. [PubMed: 28713220]

Planer-Friedrich B, London J, McCleskey RB, Nordstrom DK, Wallschlager D. Thioarsenates in geothermal waters of Yellowstone National Park: determination, preservation, and geochemical importance. Environ Sci Technol. 2007; 41:5245–5251. [PubMed: 17822086]

Rea MA, Rice RH. Telomerase deregulation in immortalized human epidermal cells: Modulation by cellular microenvironment. Int J Cancer. 2001; 94:669–673. [PubMed: 11745461]

Reznikova TV, Phillips MA, Rice RH. Arsenite suppresses Notch1 signaling in human keratinocytes. J Invest Dermatol. 2009; 129:155–161. [PubMed: 18633435]

Rice RH, Steinmann KE, deGraffenried LA, Qin Q, Taylor N, Schlegel R. Elevation of cell cycle control proteins during spontaneous immortalization of human keratinocytes. Molec Biol Cell. 1993; 4:185–194. [PubMed: 8443416]

Ritsick DR, Edens WA, McCoy JW, Lambeth JD. The use of model systems to study biological functions of Nox/Duox enzymes. Biochemical Society Symposium. 2004; 71:85–96.

Segal AW. The molecular and cellular pathology of chronic granulomatous disease. Europ J Clin Invest. 1988; 18:433–443. [PubMed: 2852593]

Shakir SK, Azizullah A, Murad W, Daud MK, Nabeela F, Rahman H, Ur Rehman S, Häder DP. Toxic metal pollution in Pakistan and its possible risks to public health. Rev Environ Contam Toxicol. 2017; 242:1–60. [PubMed: 27464847]

Song Q, Li J. A review on human health consequences of metals exposure to e-waste in China. Environ Pollution. 2015; 196:450–461.

Straub AC, Clark KA, Ross MA, Chandra AG, Li S, Gao X, Pagano PJ, Stolz DB, Barchowsky A. Arsenic-stimulated liver sinusoidal capillarization in mice requires NADPH oxidase-generated superoxide. J Clin Invest. 2008; 118:3980–3989. [PubMed: 19033667]

Sumimoto H. Structure, regulation and evolution of Nox-family NADPH oxidases that produce reactive oxygen species. FEBS J. 2008; 275:3249–3277. [PubMed: 18513324]

Swinnen I, Goossens A. An update on airborne contact dermatitis: 2007–2011. Contact Dermatitis. 2013; 68:232–238. [PubMed: 23343440]

Valencia A, Kochevar IE. Nox1-based NADPH oxidase is the major source of UVA-induced reactive oxygen species in human keratinocytes. J Invest Dermatol. 2008; 128:214–222. [PubMed: 17611574]

Wang L, Medan D, Mercer R, Overmiller D, Leornard S, Castranova V, Shi X, Ding M, Huang C, Rojanasakul Y. Vanadium-induced apoptosis and pulmonary inflammation in mice: Role of reactive oxygen species. J Cell Physiol. 2003; 195:99–107. [PubMed: 12599213]

Wickramasinghe S, Cánovas A, Rincón G, Medrano JF. RNA-sequencing: a tool to explore new frontiers in animal genetics. Livestock Sci. 2014; 166:206–216.

Yankaskas JR, Haizlip JE, Conrad M, Koval D, Lazarowski E, Paradiso AM, Rinehart CAJ, Sarkadi B, Schlegel R, Boucher RC. Papilloma virus immortalized tracheal epithelial cells retain a well-differentiated phenotype. Am J Physiol. 1993; 264:C1219–1230. [PubMed: 7684560]

Highlights

- Baseline DUOX expression in epidermal keratinocytes was maximal after confluence
- DUOX1 and 2 were stimulated by IL4, but only DUOX2 by IFNγ in epidermal keratinocytes
- In bronchial epithelial cells, IL4 induced DUOX1, while IFNγ induced DUOX2
- Vanadate markedly increased DUOX2 induction by IFNγ in epidermal keratinocytes

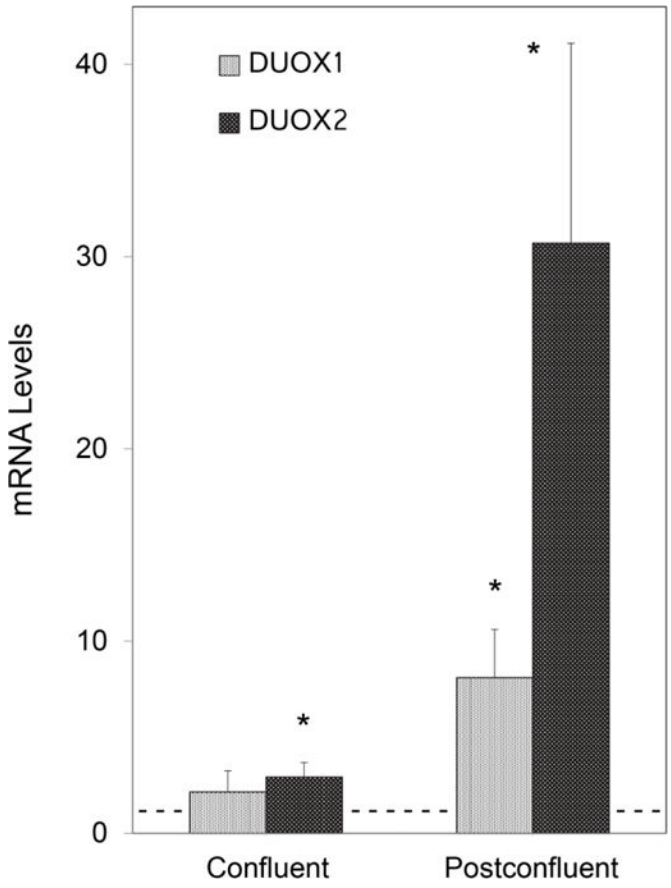

Figure 1.

Time course of DUOX expression in human keratinocytes. SIK cultures were harvested 3 days before confluence (preconfluent, mid-log phase), newly confluent and a week after confluence (postconfluent). mRNA levels were measured by real time PCR and normalized to GUSB. Shown are the combined results of 5 experiments, where the preconfluent values were set as 1. Asterisks give values significantly different ($p=0.01$ by t-test with Bonferroni correction) from preconfluence (dashed line). Ct values for the preconfluent samples were 25.3 ± 0.1 (DUOX1) and 33.5 ± 0.3 (DUOX2).

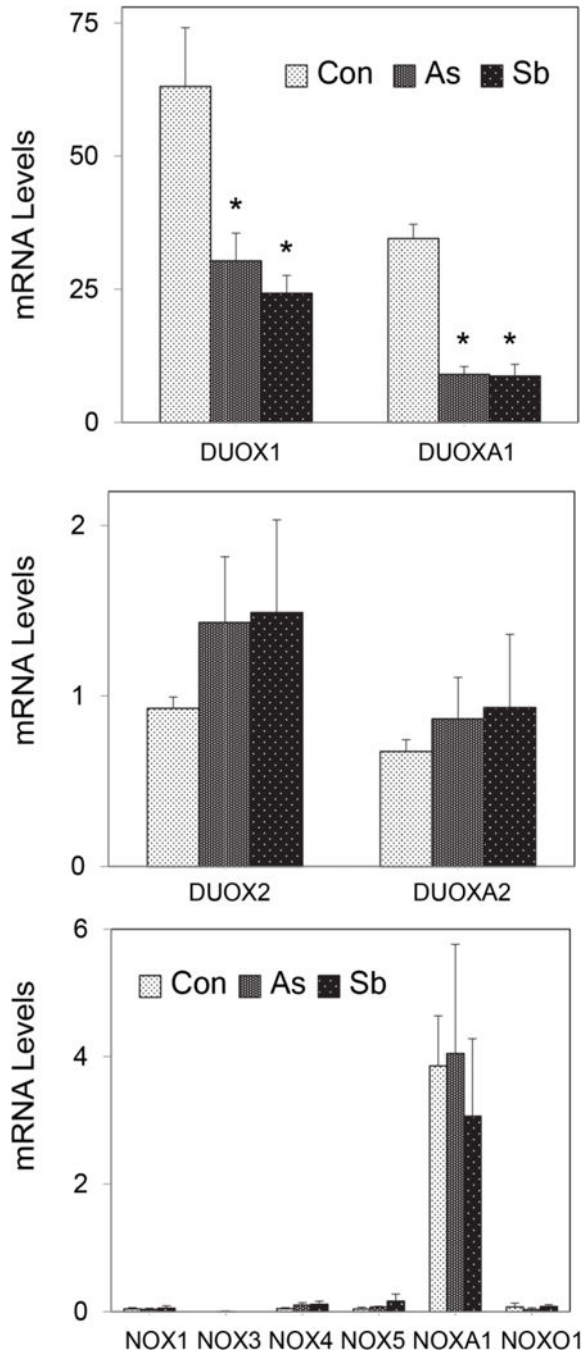

Figure 2.

Relative expression of NOX/DUOX family mRNAs in human keratinocyte culture. SIK cultures were treated with 3 μM sodium arsenite or 6 μM potassium antimony tartrate in parallel to untreated cultures for one week starting at confluence. mRNA expression, measured by next generation sequencing, is given in reads per kilobase per million mapped reads. (A) DUOX1 and DUOXA1, (B) DUOX2 and DUOXA2, (C) NOX and NOX-related mRNAs. The asterisks indicate values significantly different from untreated controls ($p<0.01$) by t-test with Bonferroni correction.

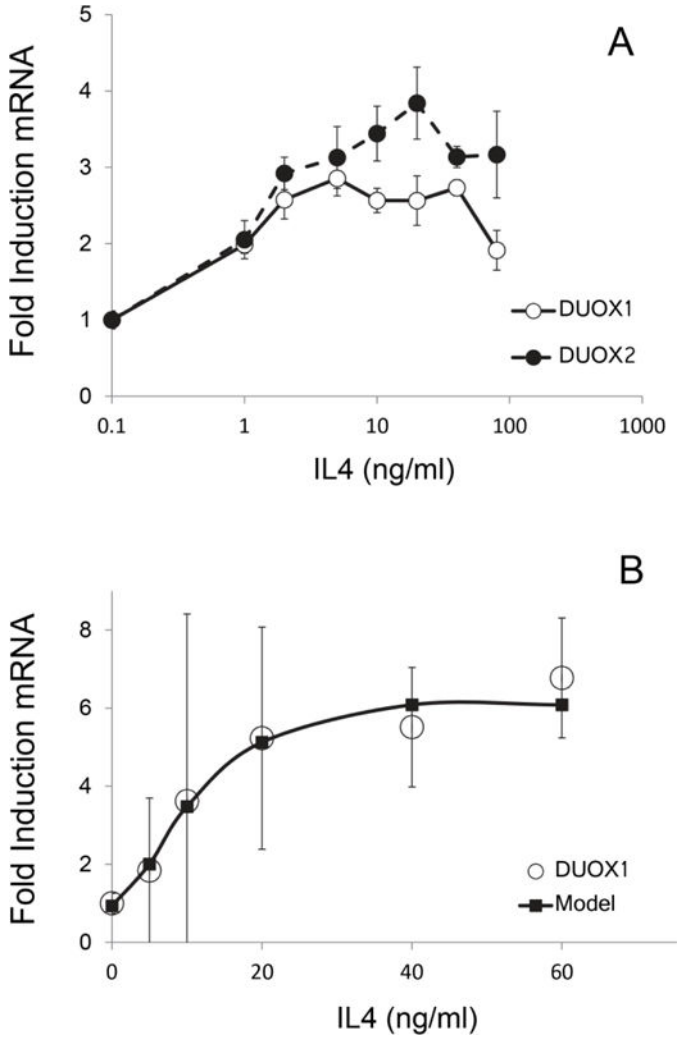

Figure 3.

Dependence of DUOX induction on IL4 concentration in (A) SIK and (B) HBE1 cultures. Illustrated in (B) are experimental data and a curve derived using Win NonLin modeling (Pharsight Software).

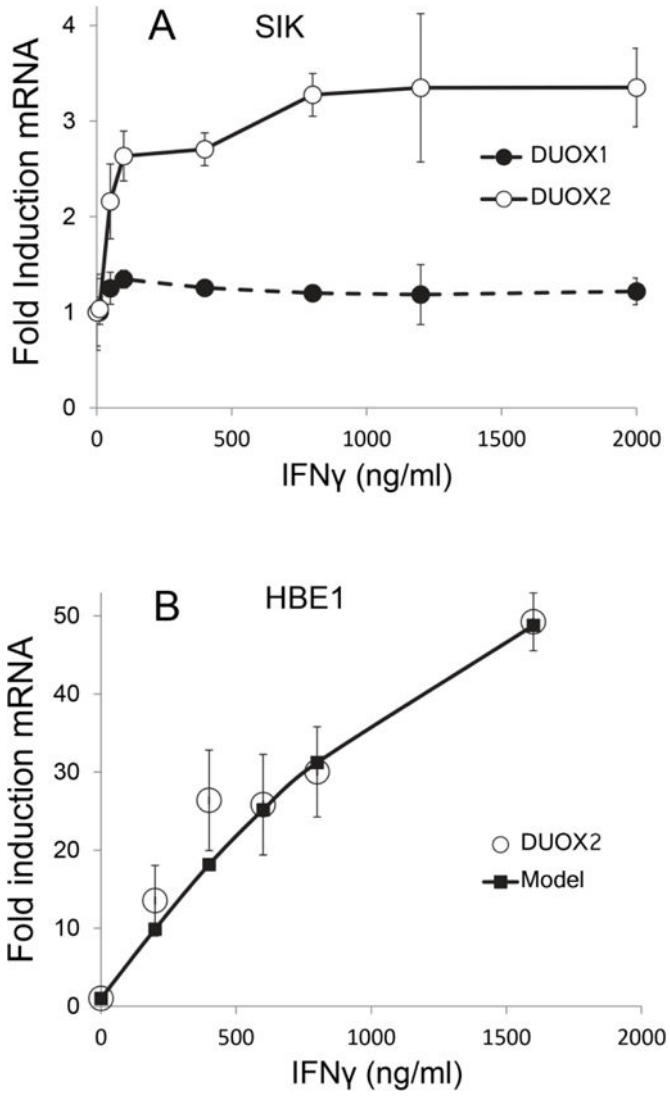

Figure 4.

Dependence of DUOX induction on IFNγ concentration in (A) SIK and (B) HBE1 cultures. Illustrated (B) are actual experimental data and a curve derived using Win NonLin modeling (Pharsight Software).

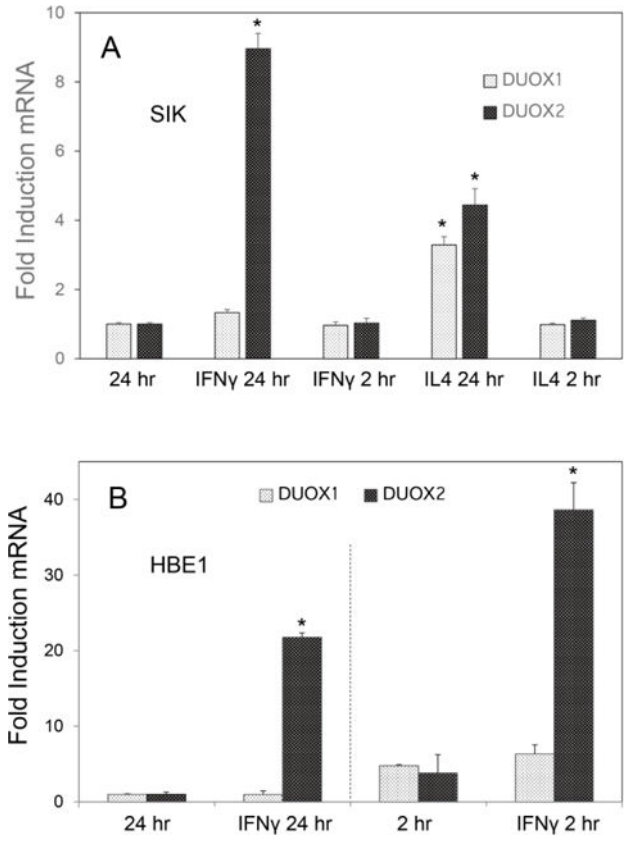

Figure 5.

DUOX induction by a 2 hour pulse or continuous exposure to IFNγ in (A) SIK or (B) HBE1 cultures. Treatments were performed at EC50 values for IFNγ, 50 ng/ml in (A) and 600 ng/ml in (B); and for IL4, 10 ng/mL in (A). Cultures were harvested and assayed 24 hr after the start of continuous treatment (24 hr) or 24 hr after completion of the 2 hr pulse (2 hr); untreated parallel cultures were harvested after 24 hr or 2 hr. In panel B, the dashed line separates cultures treated for 24 hr (left) or 2 hr (right), each with its own control, all harvested after 24 hr. Values significantly higher than no cytokine treatment (by ANOVA) are indicated by * ($p<0.01$).

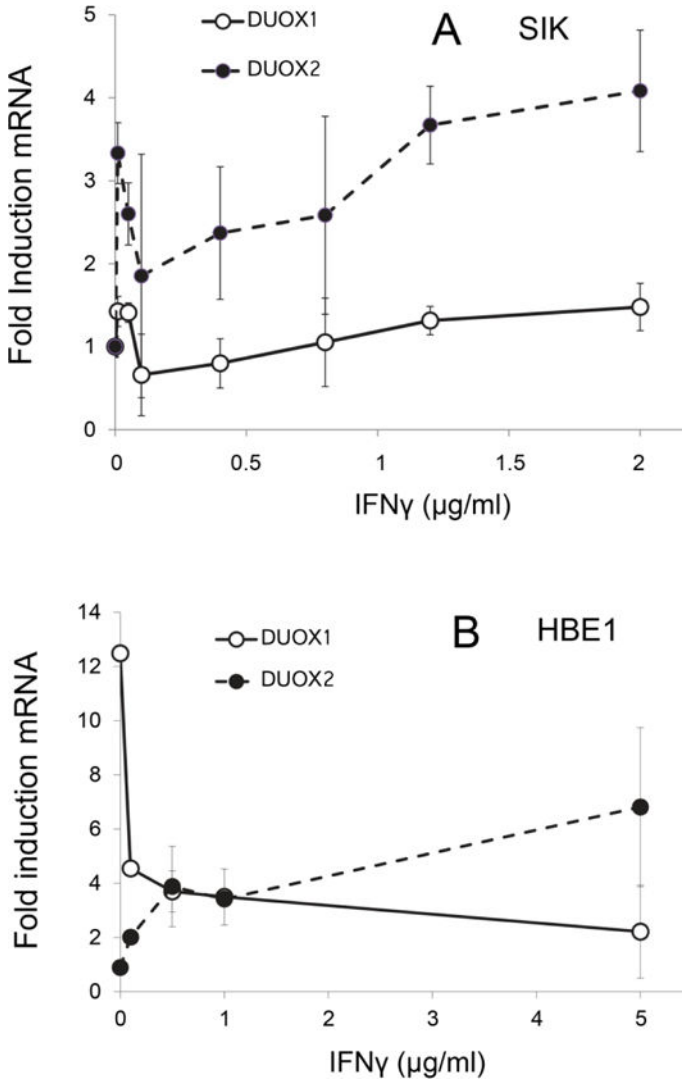

Figure 6.

Inhibition of IL4 induction of DUOX1 by IFNγ in (A) SIK and (B) HBE1. Cultures were treated with IL4 at its EC50 and the indicated concentrations of IFNγ and harvested after one day.

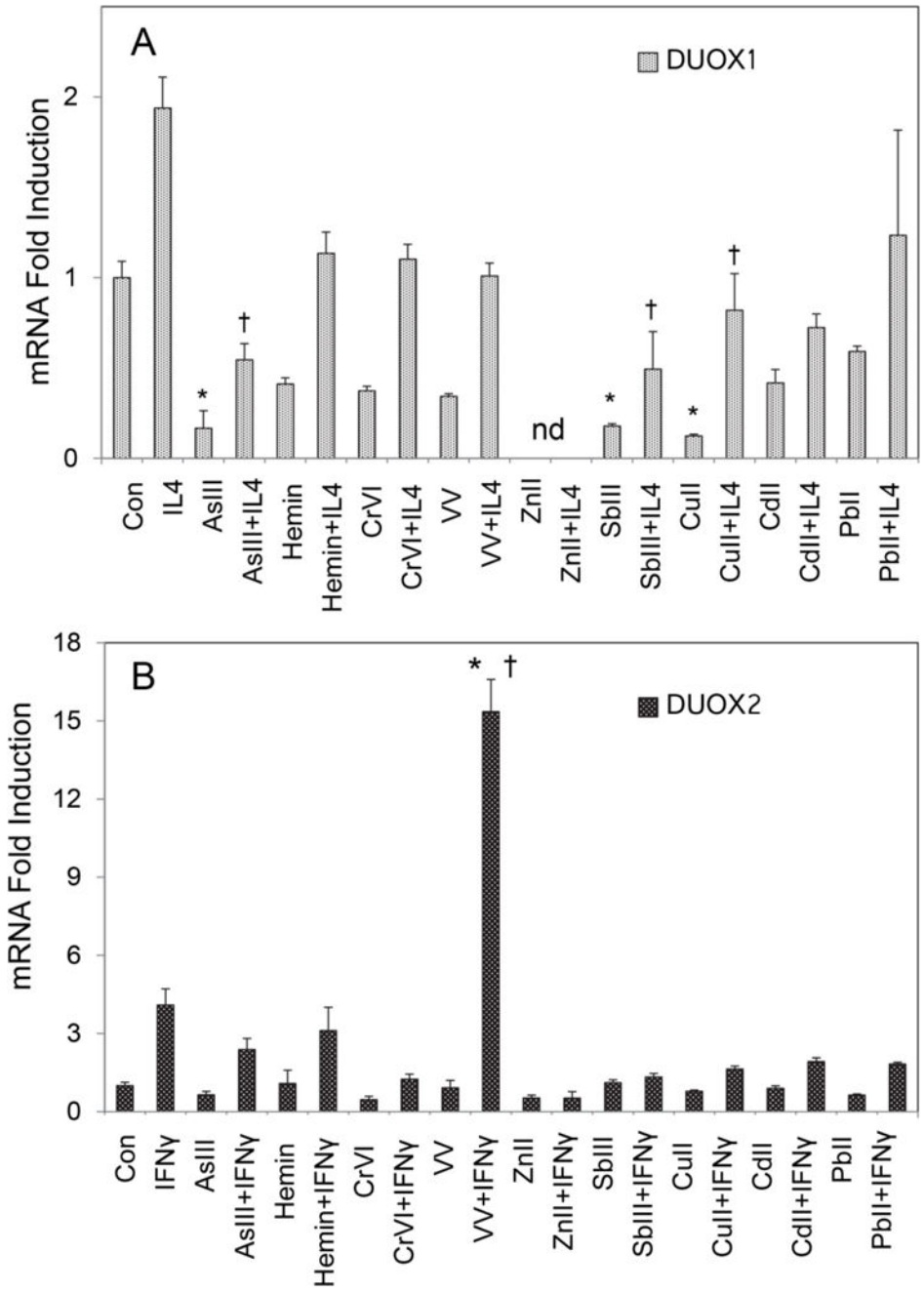

Figure 7.

Effects of metal/metalloid compounds on DUOX induction by IL4 and IFNγ in SIK cultures after 3 days of treatment. (A) DUOX1 induction by 10 ng/ml IL4 (EC50). (B) DUOX2 induction by 50 ng/ml IFNγ (EC50). Final concentrations were 2 μM $NaAsO_2$ (AsIII), 10 μM hemin, 5 μM K_2CrO_4 (CrVI), 10 μM Na_3VO_4 (VV), 100 μM $ZnSO_4$ (ZnII), 20 μM $CuSO_4$ (CuII), 10 μM $CdCl_2$ (CdII), 10 μM $Pb(NO_3)_2$ (PbII) and 5 μM antimony potassium tartrate (SbIII). nd, not determined. (A) Values for compounds alone that differed significantly from untreated controls (Con) are indicated by * ($p<0.01$), and values for compounds in the presence of IL4 that differed significantly from treatment with IL4 alone

are indicated by † ($p<0.02$); (B) values for VV+IFNγ were significantly different from those for Con (*) and VV alone (†), each $p<0.01$. Significance was calculated by ANOVA.

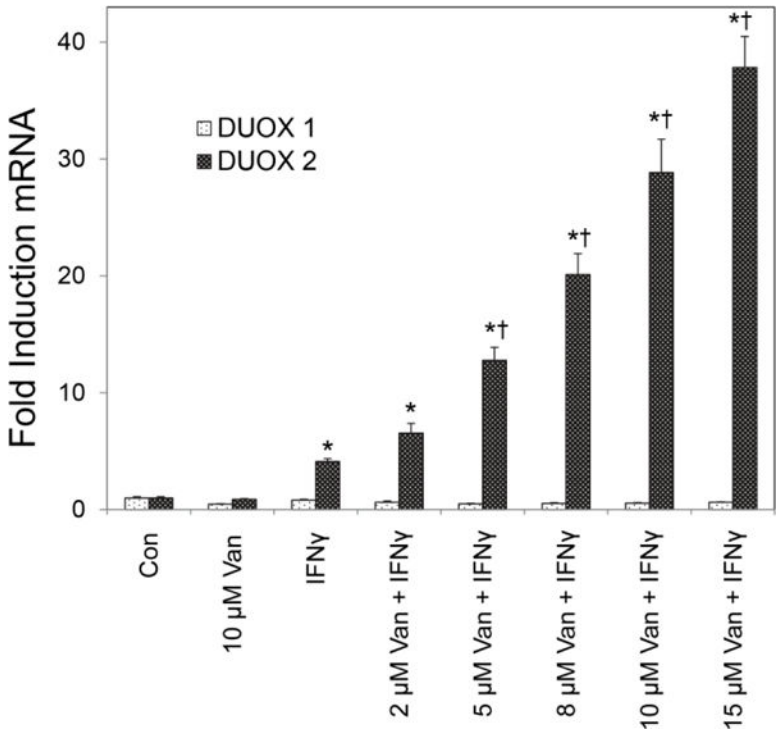

Figure 8.

Vanadate augmentation of DUOX2 induction by IFNγ at 50 ng/ml (EC50). SIK cultures were treated for 3 days with Na_3VO_4 (Van) at the indicated concentrations before IFNγ treatment. Values significantly higher than Con (*) and IFNγ alone (†), each ($p<0.01$), analyzed by ANOVA.

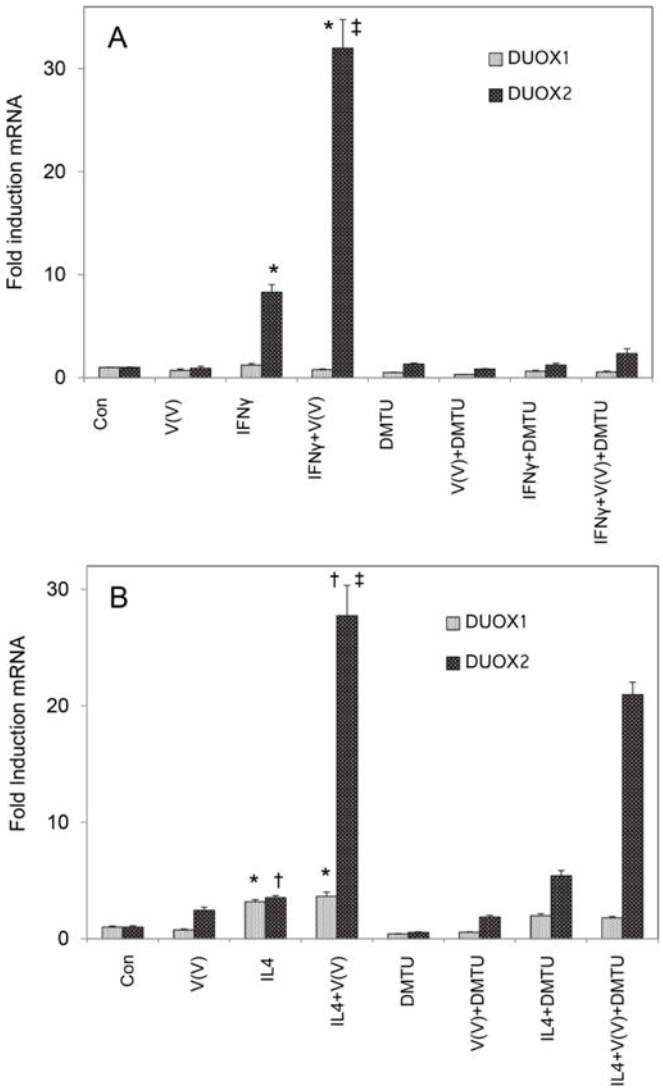

Figure 9.

Dimethylthiourea suppression of IFNγ but not IL4 action. SIK cultures were treated with dimethylthiourea (DMTU) for one hr prior to cytokine addition. The cultures were exposed to vanadate for three days; DMTU was added at the start of the third day followed one hr later by cytokine additions. (A) DUOX2 was significantly induced by IFNγ (*) compared to untreated cultures (Con), but induction was not observed in the presence of DMTU. Vanadate exposure significantly increased IFNγ induction of DUOX2 compared to Con (*) and IFNγ alone (‡), p=0.001; no significant induction in the presence of DMTU. (B) IL4 significantly induced DUOX1 above Con (*, p<0.01), not altered by the presence of vanadate. DMTU reduced the level of DUOX1 expression but did not prevent IL4 induction. IL4 stimulated DUOX2 expression with or without vanadate addition (†, p=0.003), more in the presence of vanadate than with IL4 or vanadate alone (‡, p=0.05), but DMTU did not significantly affect induction in either case. Analyzed by ANOVA.